

Motivation: The faint-end of the $z > 6$ Ly α Luminosity Function

The observable Ly α emission from galaxies during the Epoch of Reionisation depends sensitively on the residual volume averaged neutral fraction, x_{HI} , within the Universe. An observed overall decline of the Ly α emitter luminosity function (LAE LF) from $z \approx 6$ to $z \approx 7$ is linked to a rapidly decreasing $x_{\text{HI}} \rightarrow 0$ from 0.5 over $\lesssim 200$ Myr [1,2]. Consistent with other probes, we deduce that reionisation was essentially complete (i.e. $x_{\text{HI}} \approx 0$) at $z \approx 6$ [3]. Nevertheless, inferring x_{HI} solely from the integrated LAE LF is highly model dependent and current LAE samples at those epochs are limited to $\log L_{\text{Ly}\alpha} [\text{erg s}^{-1}] \gtrsim 42.3$. As of yet, we do not have strong constraints on the sub- L_* “faint-end” of the LAE LF. Interestingly, especially at sub- L_* the LAE LF is expected to show the strongest attenuation with increasing z , if reionisation proceeds “bottom-up” [4,5]. The deepest blind MUSE surveys [6-8], such as the MUSE GTO Hubble Ultra Deep Field Surveys [7,8], that encompasses the 141 h deep MUSE eXtremely Deep Field [8] (MXDF), finally allow for constraints in this respect.

A robust $z > 6$ LAE MXDF sample with LSDCat2.0

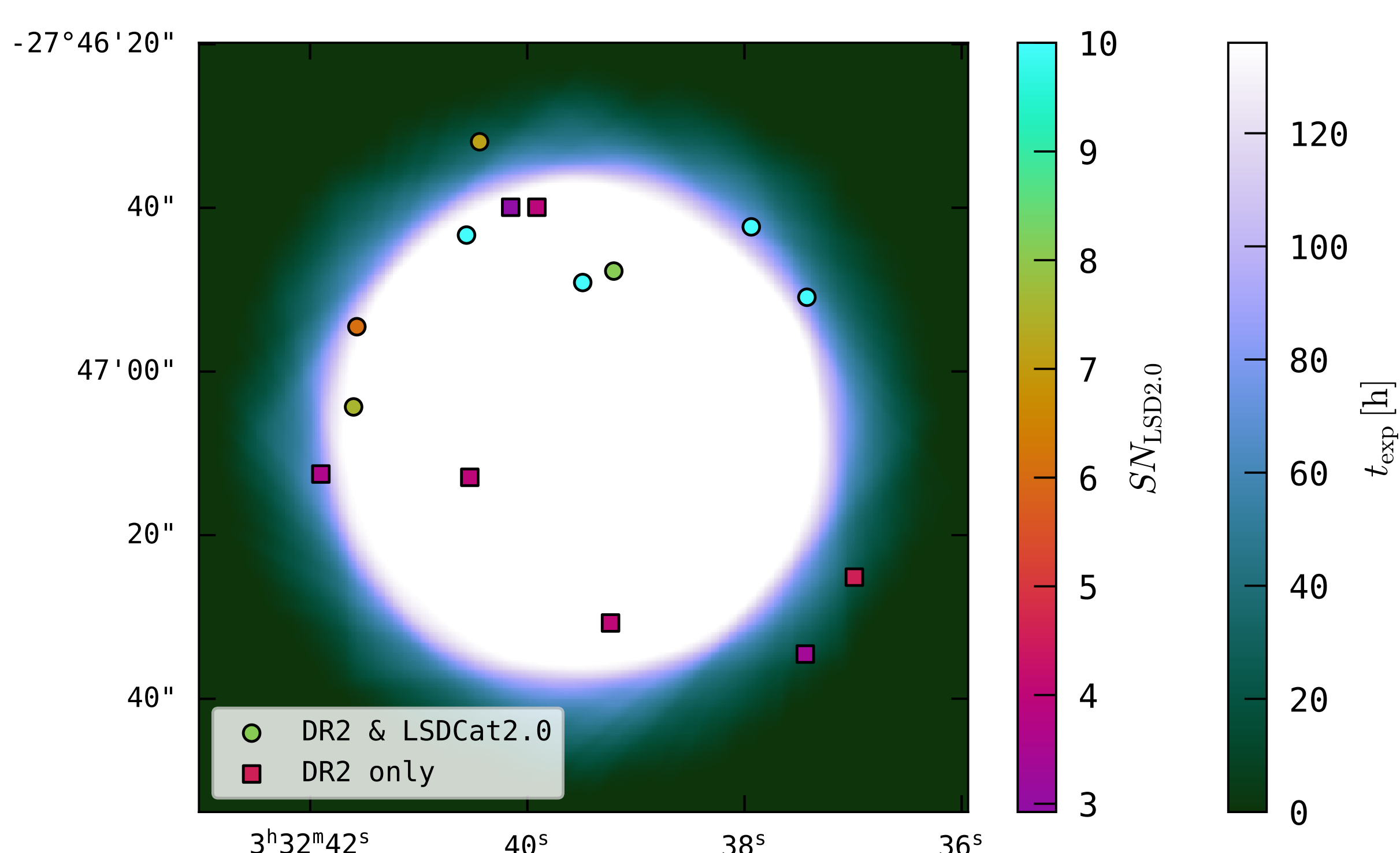


Figure 1: Positions of $z > 6$ LAEs in the MXDF, colour coded by their LSDCat2.0 matched-filter SN, plotted over the t_{exp} map. Circles correspond sources within the reference LSDCat2.0 catalogue ($\text{SN}_{\text{thresh}} > 5.4$), whereas sources only in the DR2 catalogue are shown by squares.

An unbiased census of the high- z galaxy population within the deepest MUSE fields requires a pure sample not contaminated by spurious detections and foreground galaxies with a well understood selection function. But, unfortunately the selection function of the published deep-field catalogues is unknown. Constructing a LAE sample with LSDCat2.0 [9,10] removes this problem, as the selection function of its matched filter is deterministic (see next box). To illustrate the difference between the catalogues, we compare in Figures 1 & 2 our LSDCat2.0 $z > 6$ sample to the published catalogue in the MXDF [8]. The published catalogue contains 15 $z > 6$ LAEs within the MXDF, 8 of which are recovered by LSDCat. The remaining 7 are at a lower SN, where the number of spurious detections would require significant manual cleaning of the catalogue.

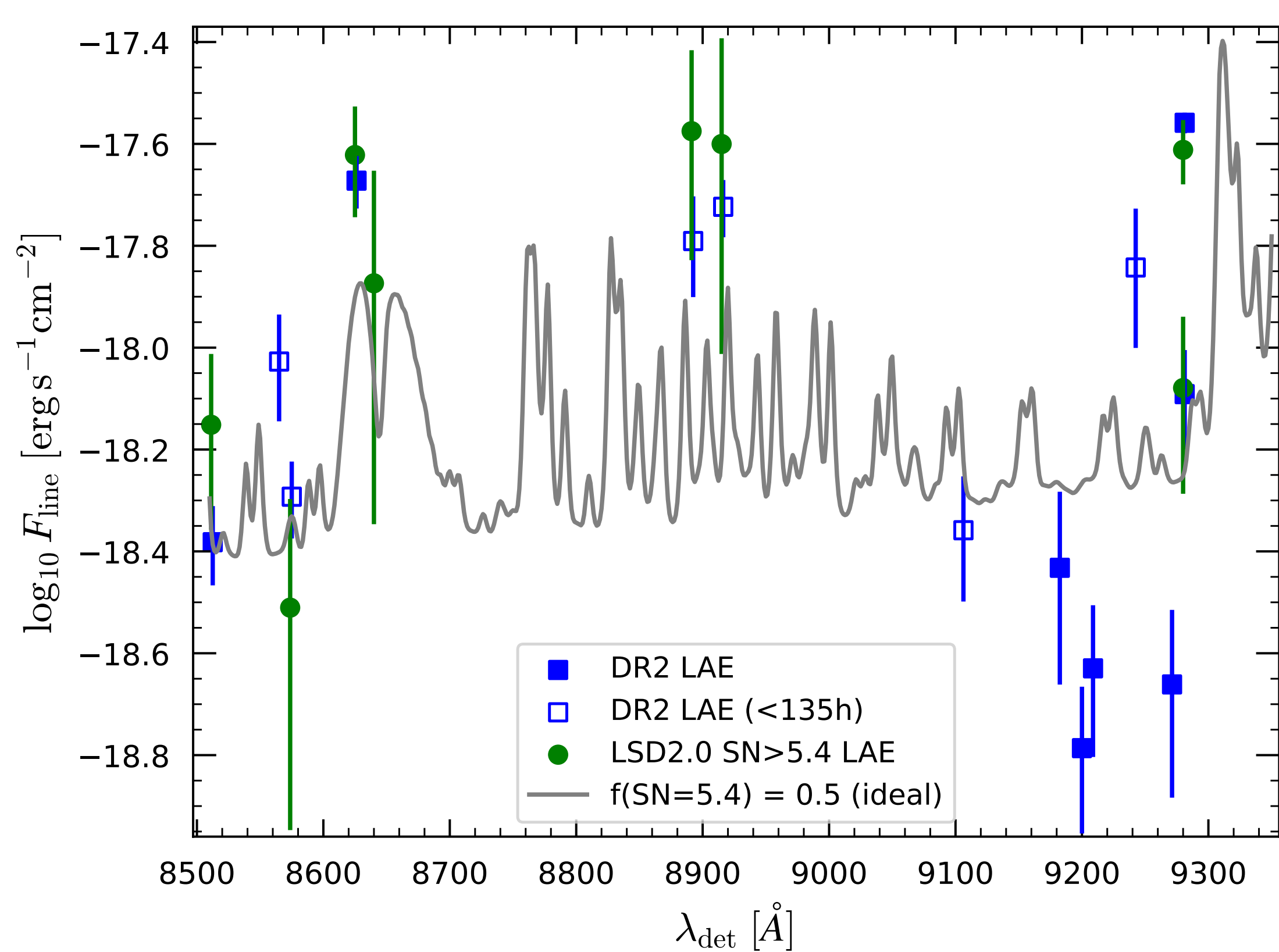


Figure 2: Line flux vs. detection wavelength of LAEs at $z > 6$ in the MXDF. Blue (open) squares show sources from DR2 (outside the deep $t_{\text{exp}} > 135$ h region), whereas LSDCat2.0 sources and measurements are shown with green circles. The grey line shows the 50% completeness limit of the idealised LSDCat2.0 selection function at $\text{SN}_{\text{thresh}} > 5.4$ (cf. Fig. 3).

(The LSDCat2.0 catalogue also contains lower z galaxies not tabulated in [8].)

The selection function for the LSDCat2.0 sample

In ref. [10] it is derived that the selection function for catalogues of line emitters constructed with LSDCat2.0, f_C , can be written as

$$f_C(F_{\text{line}}, \lambda | \text{SN}_{\text{thresh}}) = \frac{1}{2} \left[1 + \text{erf} \left(\frac{C(\lambda) \cdot F_{\text{line}} - \text{SN}_{\text{thresh}}}{\sqrt{2}} \right) \right], \quad (1)$$

where F_{line} is the emission line flux of a line at wavelength λ , $\text{SN}_{\text{thresh}}$ is the detection threshold, and $\text{erf}(x) = \frac{2}{\sqrt{\pi}} \int_0^x e^{-t^2} dt = 1 - \frac{2}{\sqrt{\pi}} \int_x^\infty e^{-t^2} dt$. The scaling factor $C(\lambda)$ in Eq. (1) depends solely on the used search template and the match between this template and the detected source. For a perfect source-template match we have

$$C(\lambda[z]) = \frac{1}{\Delta\lambda} \cdot \sqrt{\sum_{ij} (S_{ij}^{\{\lambda[z]\}})^2} \cdot \sqrt{\sum_k \frac{(S_k^{\{\lambda[z]\}})^2}{\sigma_{z-k}^2}}. \quad (2)$$

where $S_{ij}^{\{\lambda[z]\}}$ and $S_k^{\{\lambda[z]\}}$ are the spatial and spectral shapes of the 3D matched filter, respectively, σ_z^2 is the effective variance at wavelength layer $\lambda[z]$, and $\Delta\lambda$ is the spectral width of a layer in the datacube. Figure 3 compares this idealised selection function for the used Gaussian 3D search template in the MXDF [10] and $\text{SN}_{\text{thresh}} = 5.4$ to a more realistic selection function, that models the expected Ly α halos of high- z LAEs following the profiles derived in [11].

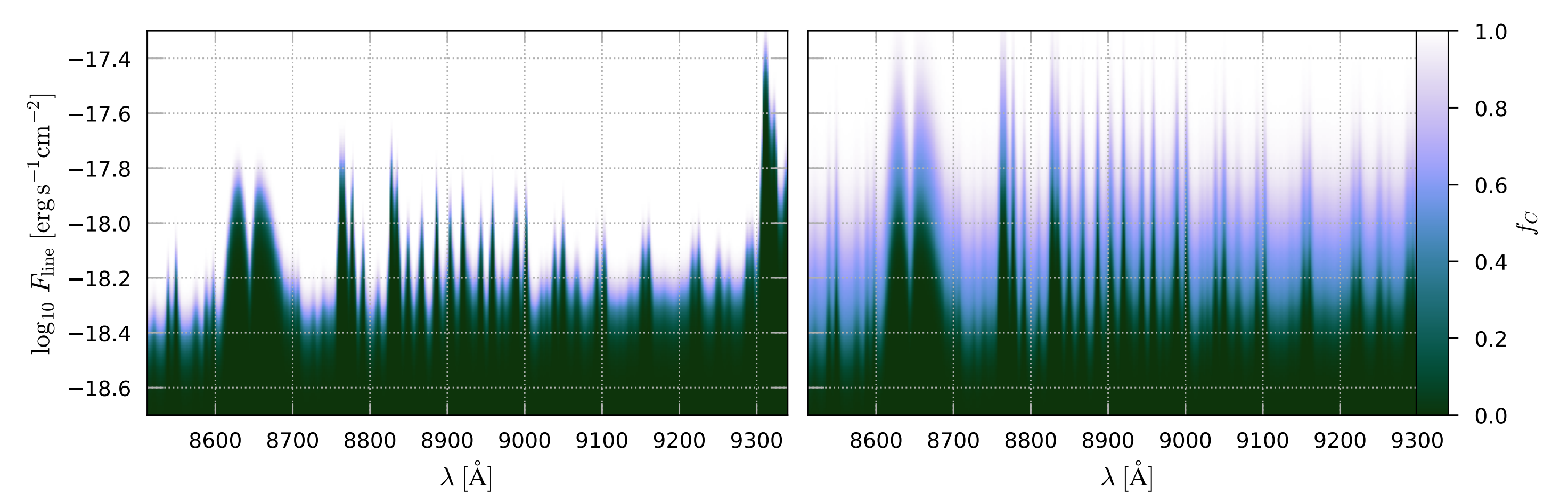


Figure 3: Comparison of the idealised selection function (left panel) to a more realistic selection function (right panel) that accounts for the expected variations in the low-SB halos of LAEs.

Faint $z > 6$ LAE number counts - expectations vs. reality

That $\log L_{\text{Ly}\alpha} [\text{erg s}^{-1}] \lesssim 41.5$ LAEs at $z > 6$ are an observationally unconstrained *terra incognita* can be appreciated when comparing number counts,

$$N_{\text{LAE}}(> F_{\text{Ly}\alpha}) = 4\pi \int_{F_{\text{Ly}\alpha}}^\infty dF \int_{z_{\text{min}}}^{z_{\text{max}}} dz \left(\frac{dV}{dz} \right)_{(z)}^{\Lambda\text{CDM}} \phi(L(F, z)) D_L(z)^2, \quad (3)$$

predicted from extrapolated Schechter LAE LF parameterisations, $\phi(L)$, from the literature [1,2,12-15]. Less than ten to more than 100 LAEs are expected at the flux limits reached in the deepest MUSE surveys, depending on the reference. We compare in Fig. 4 these expectations with the completeness uncorrected number counts of the MXDF. It becomes clear, that the completeness correction will significantly affect the outcome of LAE LFs estimated from such samples. Using the well defined f_C of samples constructed with LSDCat2.0 now finally allows to tackle this problem in a sound manner.

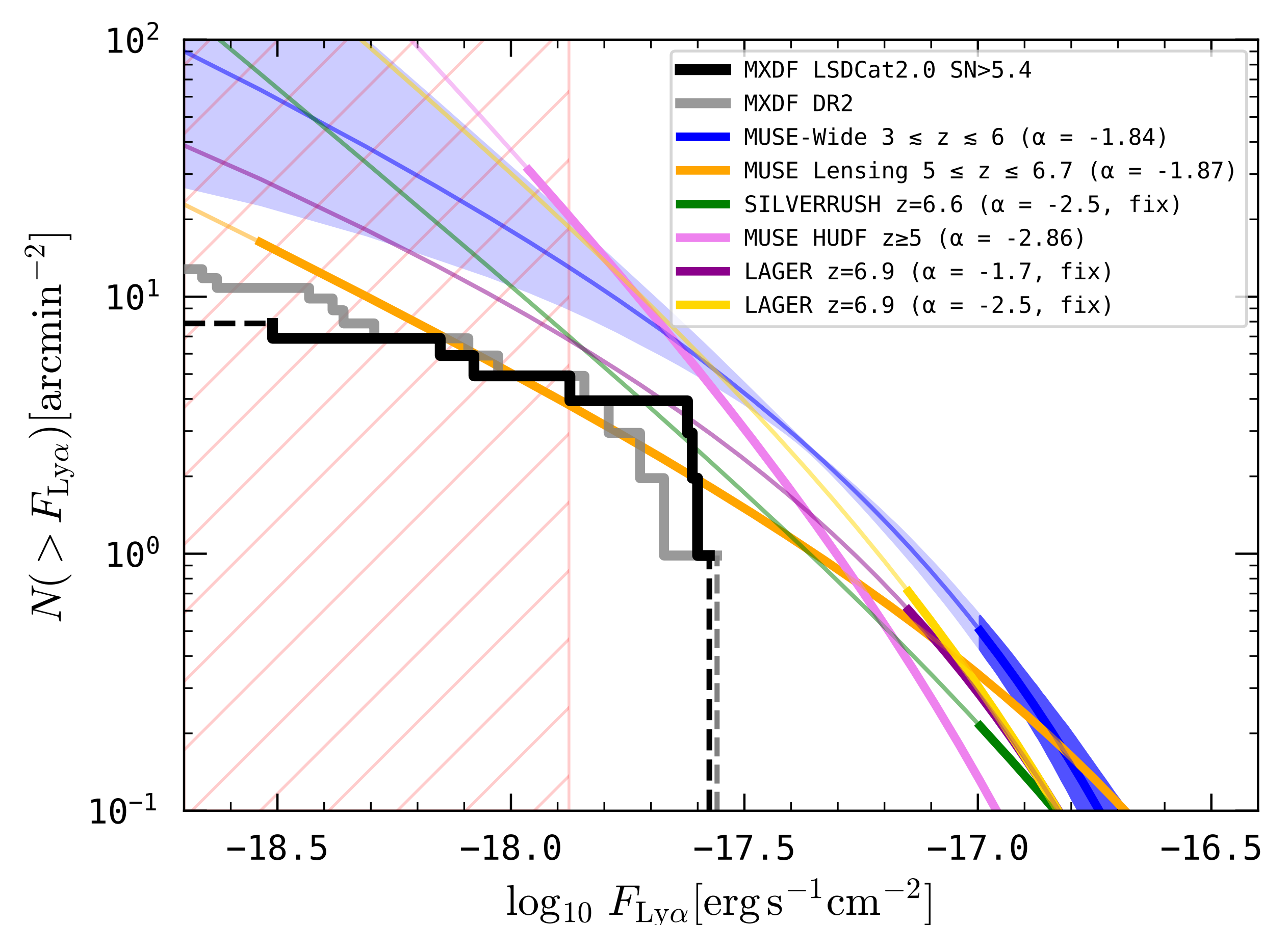


Figure 4: Number count predictions, $N(> F)$, of faint $z \gtrsim 6$ LAEs according to extrapolated Schechter parameterisations from the literature (refs. [1,2,12-15]) in comparison to completeness uncorrected number counts in the MXDF.

References

- [1] Wold, N., et al. 2022, ApJ 972, 36. [2] Konno, A., et al. 2018, PASJ 70, S16. [3] Finkelstein, S. 2016, PASA 33, e037. [4] Haiman, Z. & Cen, R., ApJ 623, 627. [5] Matthee, J., et al. 2015, MNRAS 451, 400. [6] Lusso, E., et al. 2019, MNRAS 485, L62. [7] Bacon, R., et al. 2017, A&A 608, A1. [8] Bacon, R., et al. 2023, A&A 670, A4. [9] Herenz, E.C. & Wisotzki, L. 2017, A&A 602, A111. [10] Herenz, E.C. 2023, AN (in press), e909. [11] Wisotzki et al. 2018, Nature 562, 229. [12] Herenz, E.C., et al. 2019, A&A 621, A107. [13] de La Vieuville, G., et al. 2019, A&A 628, A3. [14] Konno, A., et al. 2018, PASJ 70, S16. [15] Drake, A., et al. 2017, A&A 608, A6.